TM-1102
8035.000

Fermilab

CALCULATIONS OF PICK-UP/KICKER SENSITIVITY

David Neuffer

February 1982

In fast betatron (and momentum) cooling in the Fermilab debuncher both signal-to-noise and total power requirements are crucial design constraints[1,2] and it is important to position pick-up and kicker loops to minimize these problems. In this note we calculate the electric potential and fields for various possible pick-up/kicker placement geometries and calculate the sensitivity for these cases. Suggestions for an optimum arrangement are deduced.

I. CALCULATION OF FIELDS BETWEEN PICK-UP PLATES

The calculations in these cases reduce to solutions of electrostatic problems with various boundary conditions. Since only fields in simplified geometries are readily solvable, we will approximate physical pick-up placements by idealized geometries. The accuracy of these approximations will be discussed.

The first case we will consider was discussed by Ruggiero[3] in $\bar{p}$-148 and is shown in Fig. 1. This is the case of a charged particle between conducting plates and Sandro calculated the charge induced on the pick-up strips A and B by a unit charge at position $x = x_0$, $y = 0$. We will generalize his treatment to the case $y \neq 0$. We assume in this case and all others in this note that the fields can be approximated by a two-dimensional representation.

We consider the equation

$$\nabla^2 V = -4\pi\rho \tag{1}$$

ρ can be represented as the sum of the initial charge plus a succession of image charges

$$\rho(x,y) = \delta(x) \sum_{n=-\infty}^{\infty} \left\{ \delta(y - 2nh - y_0) - \delta(y + y_0 - (2n+1)h) \right\} \tag{2}$$

where h = g is the distance between the plates

$$\rho(x,y) = \frac{2\delta(x)}{h}\left\{\sum_{m=1}^{\infty} \cos\left(\pi(2m-1)\frac{y}{h}\right)\cos\frac{\pi(2m-1)y_0}{h}\right. \tag{3}$$

$$\left. + \sum_{n=1}^{\infty} \sin\frac{\pi(2n)y}{h}\ \sin\frac{\pi 2ny_0}{h}\right\}$$

For each m or n we find an equation

$$\frac{d^2V_m}{dx^2} - q_m{}^2V_m = -\frac{8\pi}{h}\ \delta(x)\ \cos\left(\frac{\pi(2m-1)y_0}{h}\right) \tag{4}$$

and a similar expression for V_n with a sin $q_n x$ instead of cos. The solution is

$$V_m = \frac{4\pi}{h\,q_m}\ e^{-q_m|x|}\ \cos\ [(q_m x)] \tag{5}$$

where $q_m{}^2 = \left(\frac{\pi(2m-1)}{h}\right)^2$ and $q_n{}^2 = \left(\frac{\pi 2n}{h}\right)^2$ and cos → sin for m → n,

and

$$V(x) = \sum_{m=1}^{\infty} V_m(x)\ \cos\left(\frac{(2m-1)\pi y}{h}\right) \tag{6}$$

$$+ \sum_{n=1}^{\infty} V_n(x)\ \sin\left(\frac{2n\pi y}{h}\right)$$

We want to obtain the charge on a section of width W centered at $x = x_0$. This is

$$Q = -\int_{x_0 - W/2}^{x_0 + W/2} \frac{E_y}{4\pi}\,dx \qquad \text{at } y = h/2 \tag{7}$$

$$= -\int dx\left\{\frac{1}{h}\sum_{m=1}^{\infty} e^{-q_m|x_0|}\ \sin q_m y \cos q_m y_0\right. \tag{8}$$

$$\left. - \frac{1}{h}\sum_{n=1}^{\infty} e^{-q_n|x_0|}\ \cos\ (q_n y)\ \sin q_n y_0\right\}$$

We note that

$$\sin \frac{(2m-1)\pi}{2} = (-1)^{m+1}$$

and

$$\cos \frac{2n\pi}{2} = (-1)^{n}$$

The integration over x has two possible forms:

$$\int_{|x_0| - W/2}^{|x_0| + W/2} e^{-q_n|x_0|} = \frac{1}{q_n} e^{-q_n|x_0|} 2 \sinh(q_n W/2) \tag{9}$$

if $|x_0| > W/2$, and

$$\int_{x_0 - W/2}^{x_0 + W/2} e^{-q_n|x_0|} = \frac{2}{q_n} (1 - e^{-q_n W/2} \cosh[q_n|x_0|]) \tag{10}$$

if $|x_0| < W/2$.

Thus the charge on the plate is

$$Q = \frac{2}{h} \sum_{m=1}^{\infty} (-1)^m \cos(q_n y_0) e^{-q_m|x_0|} \sinh(q_m W/2) \tag{11}$$

$$+ \frac{2}{h} \sum_{n=1}^{\infty} (-1)^n \frac{\sin}{q_n} \left(q_n y_0\right) e^{-q_n|x_0|} \sinh(q_n W/2)$$

for $|x_0| > W/2$, with a similar form for $|x_0| < W/2$. We note that the charge on the plate at $y = -h/2$ would be the same expression except the terms with $\sin(q_n y_0)$ would change sign. We consider $x_0 > W/2$ and the first sum in Eq. (11) and now reduce this to a more tractable form. The above expression can be factored into exponentials in the following form

$$+ \frac{1}{2\pi} \sum_{m-1}^{\infty} \frac{(-1)^m}{2m-1} \left[e^{\left(\frac{2m-1\pi}{h}\right)[W/2 - x_0 - iy_0]} \right] \tag{12}$$

plus three more terms. Using $\text{Atan}\,(z) = -\sum_{m-1}^{\infty} \frac{(-1)^m z^m}{(2m+1)}$

we find (11) becomes $\frac{-1}{2\pi}\,\text{Atan}\left\{ e^{-(x_0 - W) - iy_0} \right\}$ plus three more terms

Using $\text{Atan}\,(z_1) \pm \text{Atan}\,(z_2) = \text{Atan}\left[\frac{(z_1 \pm z_2)}{(1 \mp z_1 z_2)}\right]$ (13a)

and $\text{Atan}\,(1/z) = \frac{\pi}{2} - \tan z$ (13b)

we obtain (using g instead of h to agree with Ruggiero's notation)

$$Q^{++}_{upper} = \frac{-1}{2\pi} \left\{ \text{Atan} \left(\frac{\sinh\left[\frac{\pi}{g}(x_0 + W/2)\right]}{\cos \frac{\pi y_0}{g}} \right) - \text{Atan} \left(\frac{\sinh\left[\frac{\pi}{g}(x - W/2)\right]}{\cos \pi(y_0/g)} \right) \right\} \tag{14}$$

The same expression is valid if $x_0 > W/2$ and, in fact, if $|x_0| > W/2$. If $-W/2 < x_0 < W/2$ our intermediate result is

$$\frac{1}{2\pi} \left\{ -\text{Atan}\,(e^{iy}) - \text{Atan}\,(e^{-iy}) + \text{Atan}\left(e^{W/2 + x_0 + iy}\right) + 3 \text{ more terms} \right\} \tag{15}$$

The sum of the first two terms is $-\pi$. Combining all six terms using the above Atan identities obtains the result (14).

The second half of (11) can also be reduced

$$Q^{+-}_{upper} = \frac{-i}{2\pi} \sum \frac{(-1)^n}{2n} \left(e^{\frac{i2n\pi y_0}{g}} - e^{\frac{-i2n\pi y_0}{g}} \right) e^{\frac{-2n\pi x_0}{g}} \left\{ e^{\frac{2n\pi W}{2g}} - e^{\frac{2n\pi W}{2g}} \right\} \tag{16}$$

using $\ln\,(1+z) = -\sum \frac{(-1)^n}{n} z^n$, we obtain

$$Q^{+-}_{upper} = \frac{i}{\pi} \ln \left(1 + e^{\frac{-2\pi}{g} [x_0 + W/2 + i y_0]} \right) \tag{17}$$

plus three more terms.

Using the magic formula (for $z = x + iy$)

$$\arg \cosh z = \mathrm{Atan}\ (\tan y \tanh x)$$

$$= \frac{i}{2} \ln \left\{ \frac{1 + e^{-2\ (x + iy)}}{1 + e^{-2\ (x - iy)}} \right\} + 2\ iy \tag{18}$$

we can combine the four terms of equation (17) to obtain

$$Q^{+-}_{upper} = \frac{-1}{2\pi} \left\{ \mathrm{Atan} \left(\tanh \frac{\pi\ (x_0 + W/2)}{g} \tan \frac{\pi y_0}{g} \right) \right. \tag{19}$$

$$\left. - \mathrm{Atan} \left(\tanh \frac{\pi\ (x_0 - W/2)}{g} \tan \frac{\pi y_0}{g} \right) \right\}$$

When we consider a plate at $y = -g/2$, the charge is given by (15) - (19).

These expressions are the same that Tom Collins obtained for the potentials in the geometries shown in Figs. 3 and 4.[4]

Another important pick-up/kicker geometry is indicated in Fig. 5. This shows a pair of voltage difference plates between conducting plates. The potential in the rectangular gap can be calculated by a series representation. Symmetry requires that $V\ (x,y)$ be of the following form:

$$V\ (x,y) = \sum A_n \cos \left[\frac{(2n + 1)\ \pi\ x}{w} \right] \sinh \left[\frac{(2n + 1)\ \pi\ y}{w} \right] \tag{20}$$

The A_n are determined by requiring $V\ (x,\ g/2) = V_0$.

Since $1 = \frac{4}{\pi} \sum \frac{(-1)^n}{2n+1} \cos\ (2n + 1)\ \bar{x}$ if $(|\bar{x}| < \pi/2)$, we find

$$A_n = \frac{4\ V_0\ (-1)^n}{\pi\ (2n + 1) \sinh \left(\frac{\pi g}{2w}\right)} \tag{21}$$

The fields E_y and E_x are found from the derivatives of V and are shown in Fig. 4.

The conducting plates next to the pick-up/kicker plates, as shown in Figs. 1-3, seriously distort fields near the intersection of the active and passive plates.

This distortion is particularly serious in the difference signal of Fig. 6 (or Fig. 4). Greater sensitivity is possible with a non-conducting gap between the plates. Umallotti at CERN has solved for the fields in such a geometry[5] and his solution is displayed in Fig. 7. Note that this solution uses the complex variable technique.

II. CALCULATIONS OF SENSITIVITY

In this section we present results of numerical calculations of pick-up/kicker sensitivity for various possible geometries.

As we noted above, the charge induced on the pick-up plates is proportional to the voltage induced at the beam particle position by a voltage on the pick-up plates. We are interested in the dependence of this charge on particle position; therefore, the sensitivity is proportional to the derivative of the voltage, the E-field.

The kick applied to the particle also directly depends on the field induced by the plate voltages. Thus the sensitivity of the kicker is also determined by the E-fields at the kicker.

In this note we compare sensitivity with an "ideal" pick-up/kicker - a set of difference plates of infinite extent with constant field $2V_0/h$ where $\pm V_0$ is the plate voltage and h is the distance between the plates. (See Fig. 2.)

We also decouple x and y motion in these calculations, although our calculations indicate that these couplings are of some importance in the nonlinear regions of the pick-up/kickers.

The first geometry we consider in some detail is shown in Fig. 7 and consists of four plates. The difference between top and bottom plates provides y cooling; the difference between left and right plates provides x cooling.

The fields from equations (14) and (19) can be used to calculate the fields and sensitivities. Figures 8, 9, 10 show some results of these calculations. Sensi-

tivities are calculated using fields along the x-axis (y=0) since the y dependence is much less. For difference sensitivity Eq. (22) (Fig. 7) is used rather than (19), which assumes that the gap between A and B and C and D can be non-conducting.

In this geometry the requirements of x and y cooling conflict to some extent. y cooling is optimum if the gap between plates A and B is zero, x cooling is optimum if the gap is the beam size.

Figure 10 shows a near-optimum balance between x and y cooling requirements and the power requirements are similar to that of reference 1. (See below.) Figure 8 is rejected since the 4 cm plate width is considered too long for our 2-4 GHz debuncher cooling.

The second geometry we explore is the "box" geometry of Fig. 5. We are particularly interested in the effects of the side plates on the gap fields to test the feasibility of the debuncher x-y pick-up/kicker geometry shown in Fig. 11. (x cooling is provided by the difference between plates B and D, y cooling by plates A and C.)

We have calculated the fields in three possible geometries: $g = 0.5w$, $g = w$, $g = 1.5w$. The first case is substantially the same as the ideal parallel plate case of Fig. 2, there are no large nonlinearities. The fields for the last two cases are exhibited in Figs. 12 and 13.

The nonlinearities in Fig. 12 appear to be reasonably small if the beam is confined to the region $x^2 + y^2 < \frac{1}{2}\left(\frac{g^2}{2}\right)$.

For the case of Fig. 13 ($g = 1.5w$) the nonlinearities are substantially larger and cooling is significantly suppressed. This case corresponds to debuncher x cooling in the case where x and y pick-ups are in a box geometry in a high dispersion straight section.

A comparison between the case of Fig. 13 and the case of Fig. 10 indicates that x-y transverse cooling is better with the 4-plate geometry of Fig. 10 than with the box of Fig. 13. The square "box" configuration of Fig. 12 has superior sensitivity to both of these (13, 10) but is suitable only for a zero dispersion straight section.

Another important result of this analysis is the requirement that the width of the vacuum chamber in a pick-up/kicker array be greater than the pick-up/kicker separation.

III. IMPLICATIONS FOR DEBUNCHER COOLING

In our previous paper, we calculated parameters for debuncher cooling in the case in which both x and y pick-ups are difference pick-ups in separate straight sections with a sensitivity $\bar{S} = .77 = \sqrt{0.6}$ in agreement with that expected for a simple difference PU/K (see Fig. 14).

We now consider the case where the pick-up/kickers are in the 4-plate geometry of Fig. 7, as calculated for the cases of Figs. 8-10. The sensitivities must be averaged over the full particle distribution. In averaging over both pick-up and kicker, it must be noted that because of the 90° phase shift between them, a particle will be in different sensitivity regions. (In fact a particle in a lower sensitivity region at the pick-up should be in a high sensitivity region at the kicker and vice versa.) This should smooth out sensitivity variations.

In Table I we compare sensitivities for cases 8-10. We have assumed that the noise does not depend on the PU/K geometry. We find, typically, less sensitivity and greater power requirements with the 4-plate geometry which is less sensitive than the difference plates.

Case 8 is found unacceptable because the plates are "too wide," 4 cm is greater than their length (2.5 cm).

Case 10 obtains the same power requirements as Ref. 1 by reducing the gap from 4 cm to 3.333, which reduces the safety factor from $\sqrt{2}$ to 1.2. Some reduction could also be obtained with Ref. 1, but perhaps not as much, since in the 4-plate geometry the region directly above the beam is vacant.

Power requirements have been estimated by using the noise-limited formula for the power from Ref. 1

$$P = \frac{2}{R^2}\left(\frac{E_0}{e}\right)^2 \frac{kT\ W\ g^2}{e^2\ N^2\ f_0^2\ \ell_k}\left(\frac{\varepsilon}{\pi}\right)^2\left(\frac{F}{\bar{S}}\right)^4 \frac{1}{n_k\ n_p}$$

(Note that our $\bar{S}$ is $\sqrt{S}$ of Ref. 1.)

The parameters we have chosen are the same as in Ref. 1 and are defined there.

Since the PU/K occupy only two debuncher straight sections each it is fairly easy to add, say, two more to obtain 512 PU/K and power demands of 80W for y, 300W for x with slightly better cooling.

Another possibility would be to have dispersion-free straight sections with difference PU/K. This will make x and y power requirements equal at ~200W with 256 PU/K.

REFERENCES

1. Fast Transverse Cooling in the Debuncher, D.Neuffer, 12/9/81 (unpublished).

2. Parameters for Fast Betatron Cooling in the Fermilab Debuncher, D.Neuffer, 11/17/81, ($\bar{p}$ note).

3. A.Ruggiero, $\bar{p}$ – 148

4. T.Collins, private communication.

5. Umallotti, unpublished communication.

TABLE I

COMPARISON OF POWER REQUIREMENTS OF COOLING SCENARIOS

	Ref.1	Case 8	Case 9	Case 10
N_{PU}/N_K number of PU/K	256	256	256	256
$\bar{S}_x$	.54	.53	.42	.45
$\bar{S}_y$	.77	.59	.66	.63
g cooling gain	.015	.015	.015	.015
F (aperture safety factor)	1.4	1.4	1.4	1.2
Power (y cooling)	∿200W	600W	450W	260W
Power (x cooling)	∿1000W	1000W	2530W	1000W
Vertical cooling	$(20\pi\rightarrow7\pi)$V	$20\pi\rightarrow7\pi$	$20\pi\rightarrow7\pi$	$20\pi\rightarrow7\pi$
Horizontal cooling	$(20\pi\rightarrow8\pi)$H	$20\pi\rightarrow8\pi$	$20\pi\rightarrow9\pi$	$20\pi\rightarrow8\pi$
PU/K width	2 cm plates	4 cm plates	2 cm plates	2 cm

FERMILAB
ENGINEERING NOTE

SECTION	PROJECT	SERIAL-CATEGORY	PAGE

SUBJECT: Image Charges Fig. 2A

NAME

DATE

REVISION DATE

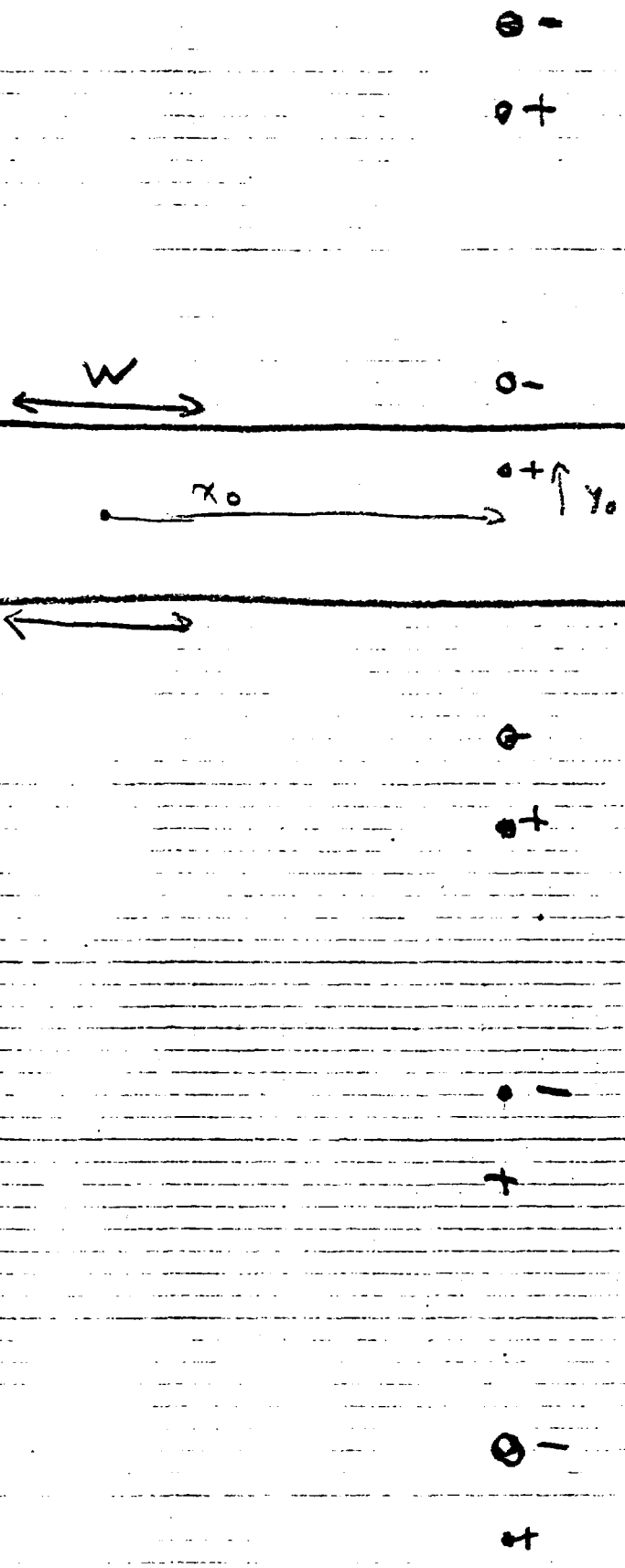

FERMILAB
ENGINEERING NOTE

SECTION	PROJECT	SERIAL-CATEGORY	PAGE

SUBJECT: Fig. 2B

NAME:

DATE:

REVISION DATE:

Ideal difference pick up

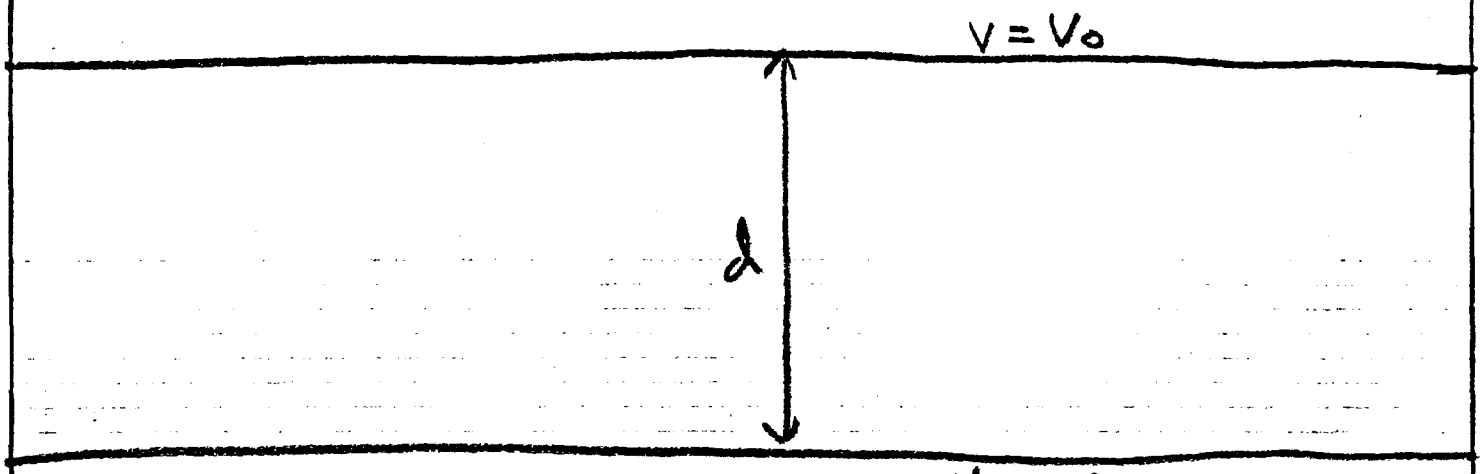

$E_y = 2 \cdot V_o / d$

$E_x = 0$

FERMILAB
ENGINEERING NOTE

SECTION	PROJECT	SERIAL-CATEGORY	PAGE

SUBJECT: Figure 3 Potentials on Sum plates

NAME:

DATE: REVISION DATE:

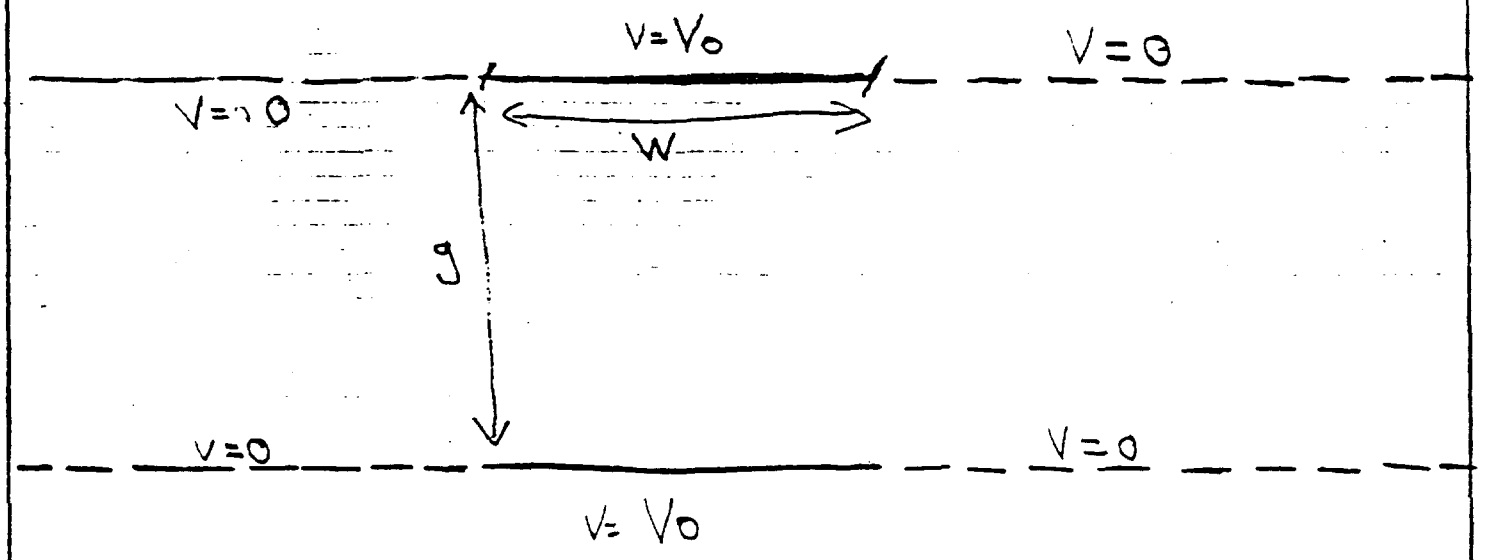

$$V = \frac{V_0}{\pi}\left\{ \mathrm{Atan}\left(\frac{\sinh \frac{\pi}{g}\left(x_0 + W/2\right)}{\cos \frac{\pi y_0}{g}}\right) - \mathrm{Atan}\left(\frac{\sinh \frac{\pi}{g}\left(x_0 - W/2\right)}{\cos \frac{\pi y_0}{g}}\right)\right\}$$

FERMILAB
ENGINEERING NOTE

SECTION	PROJECT	SERIAL-CATEGORY	PAGE

SUBJECT: Figure 4 Difference Potential

NAME:

DATE:

REVISION DATE:

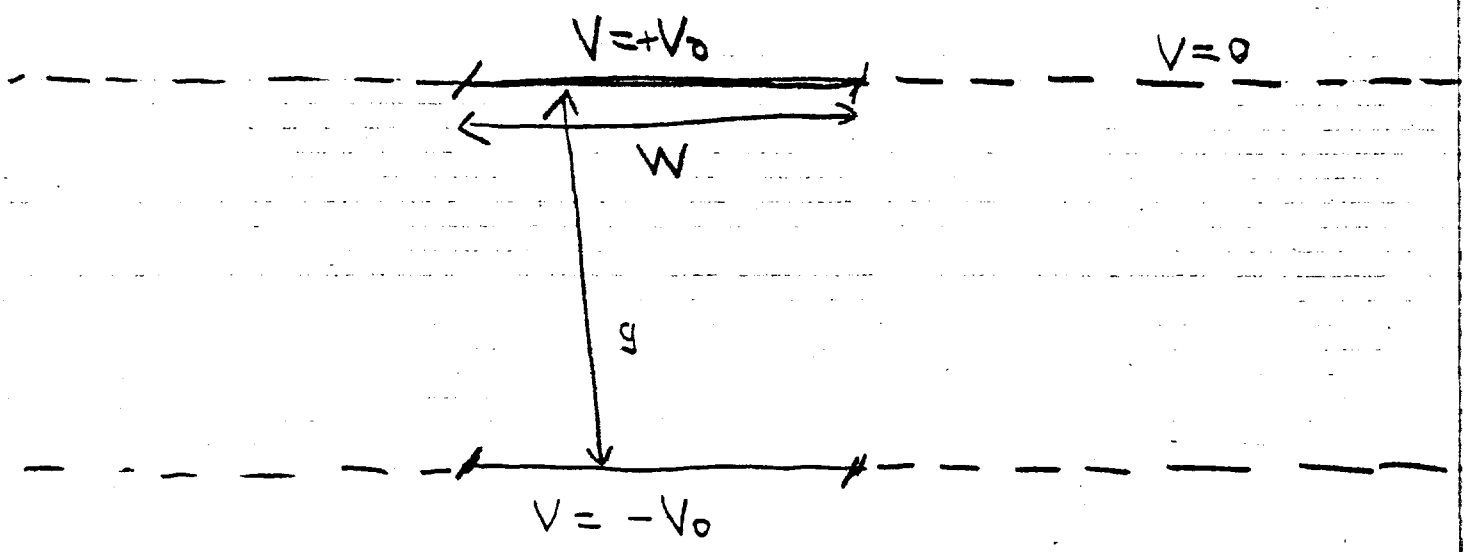

$$V = \frac{V_0}{\pi}\left\{ \mathrm{Atan}\left(\tanh \frac{\pi}{g}\left(x_0 + W/2\right) \tan \frac{\pi y_0}{g}\right) - \mathrm{Atan}\left(\tanh \frac{\pi}{g}\left(x_0 - W/2\right) \tan \frac{\pi y_0}{g}\right)\right\}$$

Figure 5:

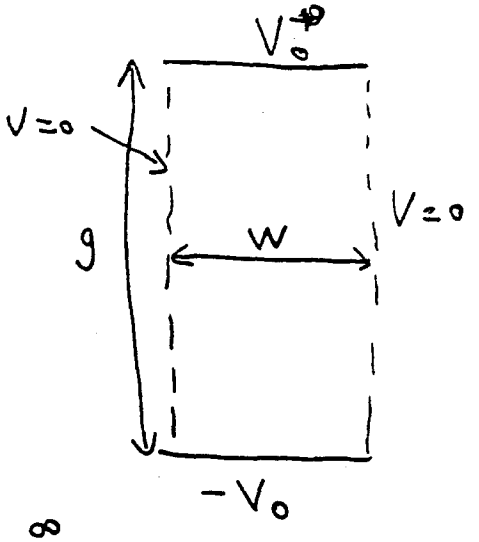

$$V(x,y) = \frac{4V_0}{\pi}\sum_{n=0}^{\infty}\frac{(-1)^n}{2n+1}\,\frac{\cos\left[\frac{(2n+1)\pi}{w}x\right]\sinh\left[\frac{(2n+1)\pi}{w}y\right]}{\sinh\left[\frac{(2n+1)\pi g}{2w}\right]}$$

$$E_x = \frac{4V_0}{w}\sum_{n=0}^{\infty}(-1)^n\,\frac{\sin\left[\frac{(2n+1)\pi x}{w}\right]\sinh\left[\frac{(2n+1)\pi y}{w}\right]}{\sinh\left[\frac{(2n+1)\pi g}{2w}\right]}$$

$$E_y = -\frac{4V_0}{w}\sum_{n=0}^{\infty}(-1)^n\,\frac{\cos\left[\frac{(2n+1)\pi x}{w}\right]\cosh\left[\frac{(2n+1)\pi}{w}y\right]}{\sinh\left[\frac{(2n+1)\pi g}{2w}\right]}$$

FERMILAB
ENGINEERING NOTE

SECTION	PROJECT	SERIAL-CATEGORY	PAGE

SUBJECT: Fields for difference PU/K
Figure 6

NAME: D Neuffer
DATE:
REVISION DATE:

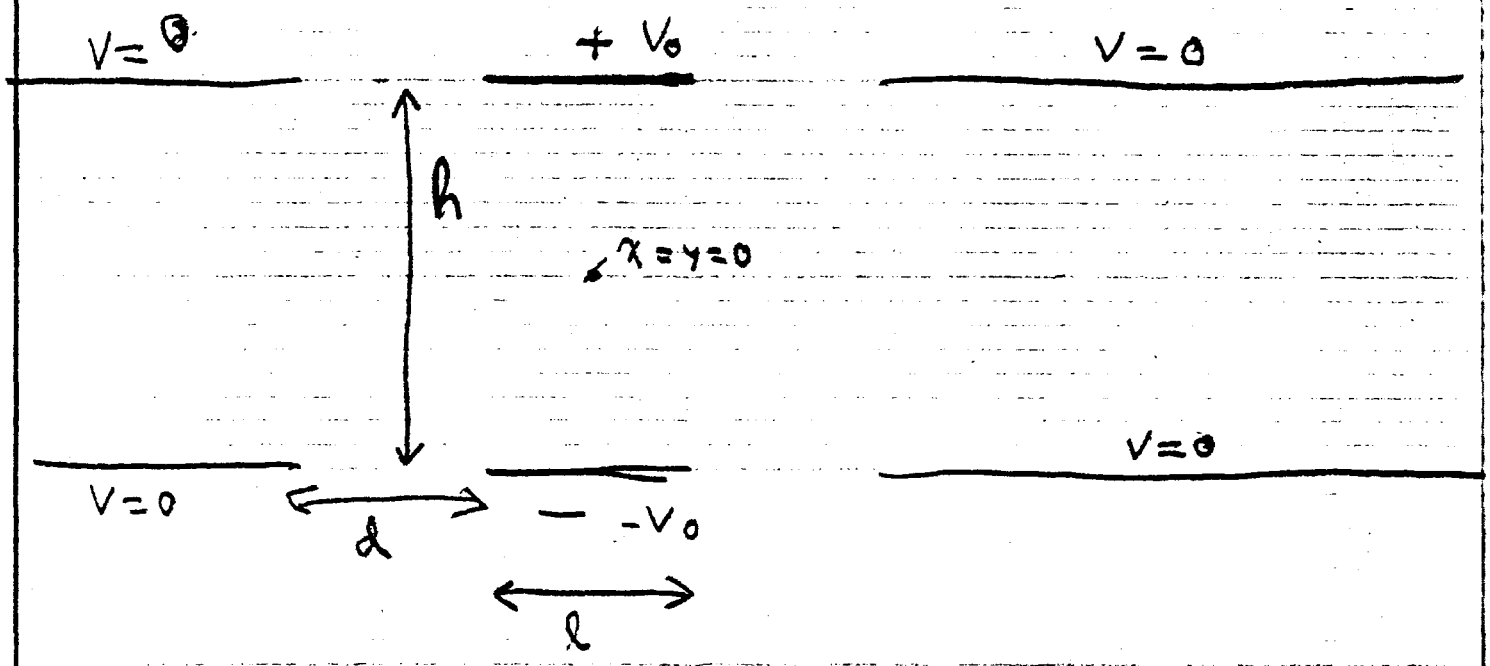

$$E_y \pm i E_x = \left\{ \frac{C(1-t)}{\sqrt{(a-t)(b-t)}} \right\} \qquad (22)$$

$$a = \frac{1}{\tanh^2\left(\frac{\pi}{h}\left(d + \ell/2\right)\right)}$$

$$b = \frac{1}{\tanh^2\left(\frac{\pi \ell}{2h}\right)} \qquad t = \tanh^2\left(\frac{\pi z}{h}\right)$$

where $z = x + iy$

$$C = \frac{\pi\sqrt{b}}{K(1-a/b)} \cdot \frac{V}{h}$$

$K(1-a/b)$ is a complete elliptic integral

Electric fields are obtained by evaluation of a <u>complex</u> quantity.

figure 7 - 4-plate sensitivity

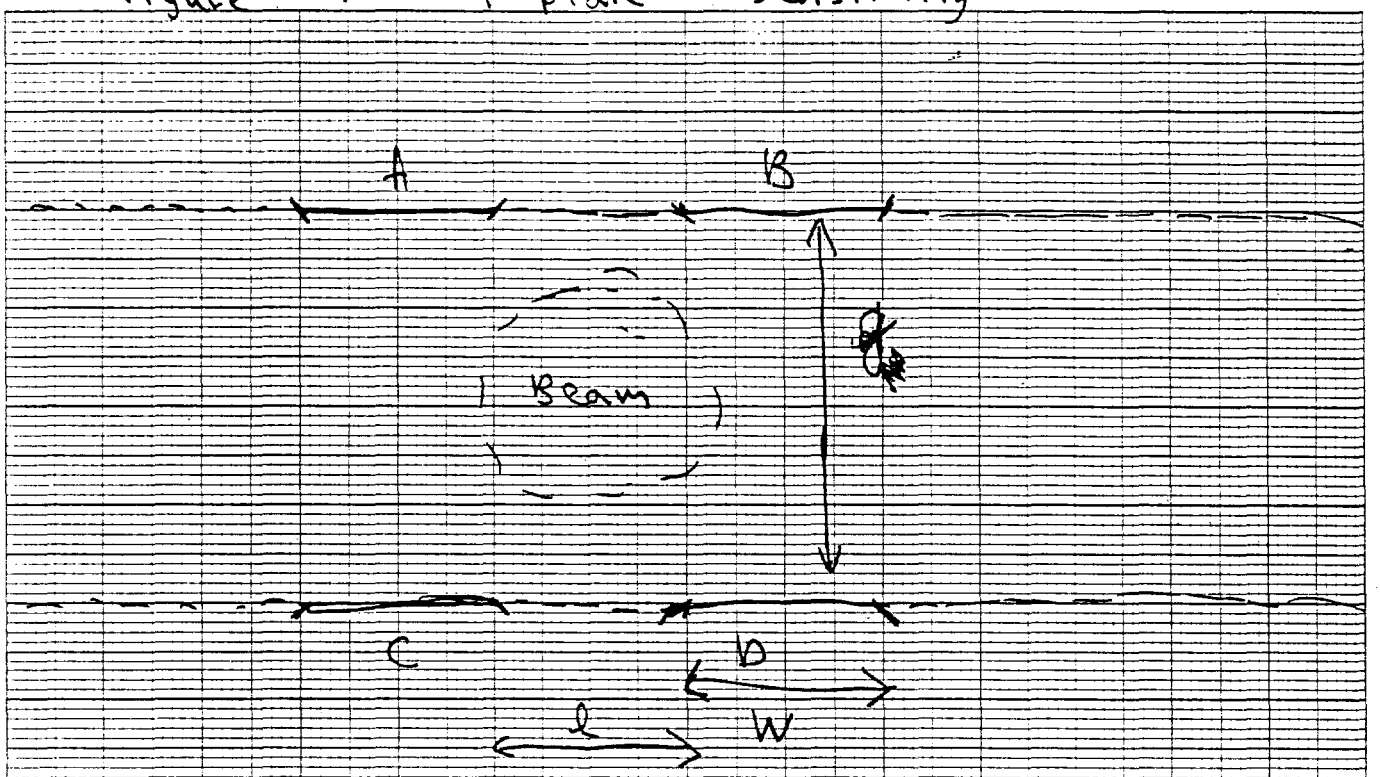

figure 9

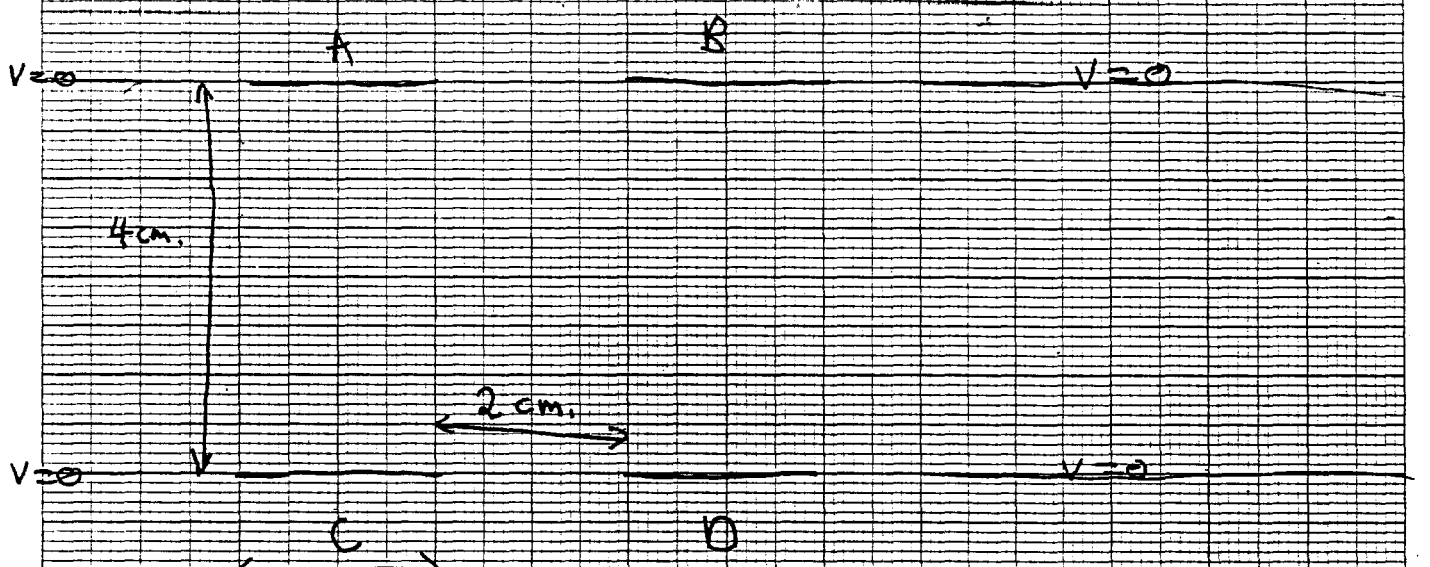

$\overline{S_y} = .66$

$\overline{S_x} = .42$

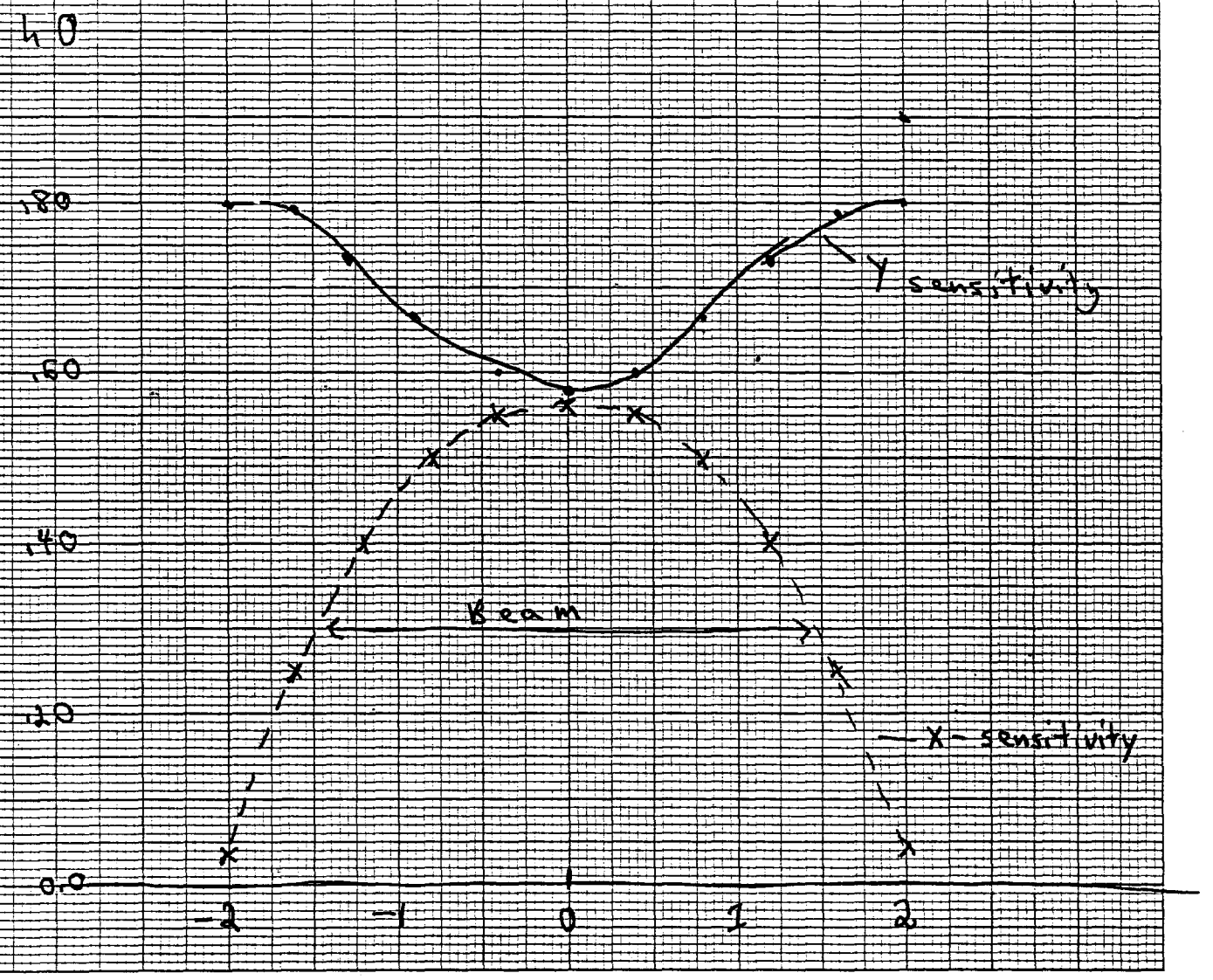

Figure 10

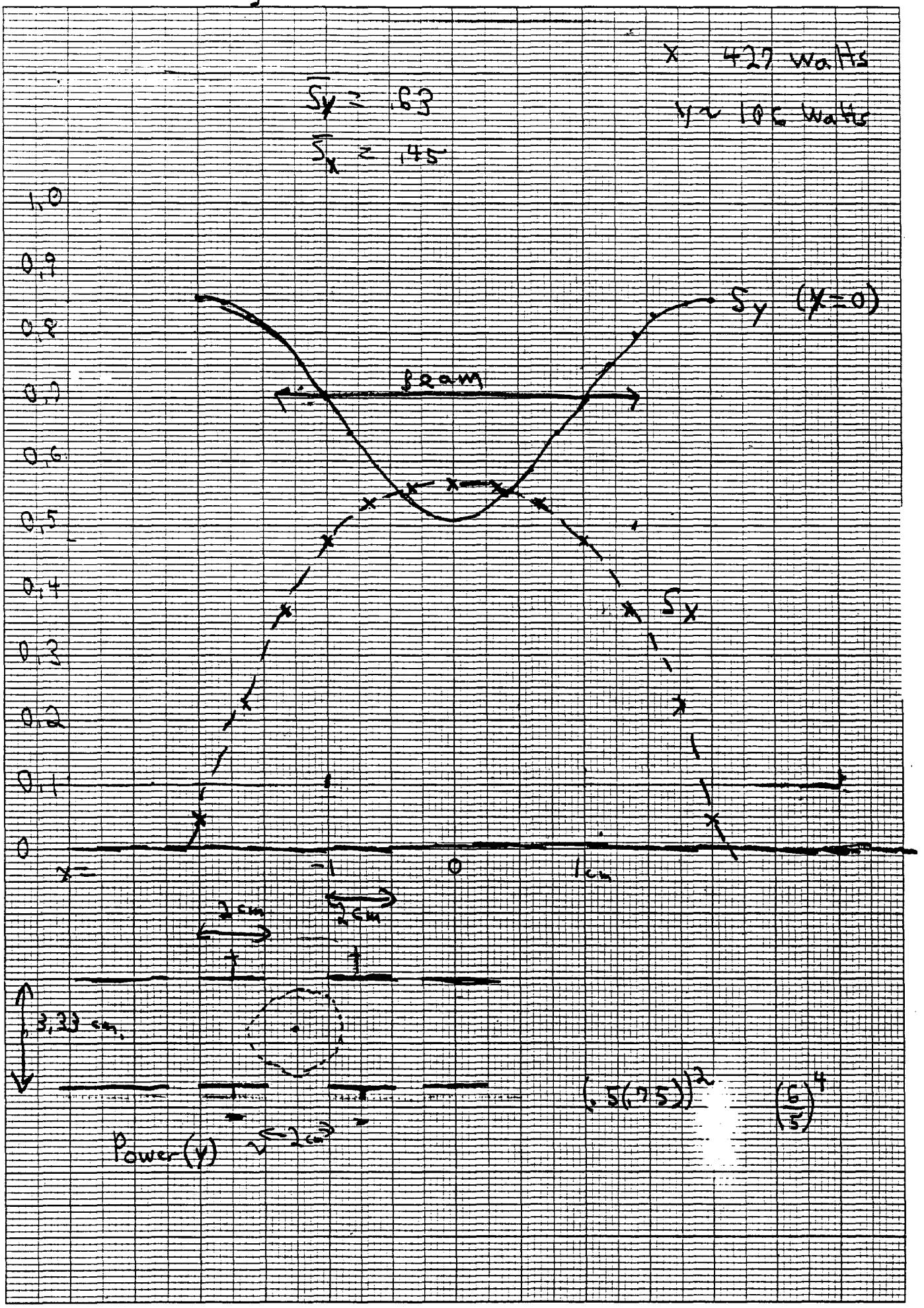

x 427 Watts
y ~ 106 Watts
$\bar{S}_y$ = .63
$\bar{S}_x$ = .45
1.0
0.9
0.8
0.7
0.6
0.5
0.4
0.3
0.2
0.1
0
S_y (y=0)
beam
S_x
x =
-1
0
1cm
2cm
2cm
3.33 cm.
$(.5(.75))^2$
$\left(\frac{6}{5}\right)^4$
Power(y)
2cm

FERMILAB
ENGINEERING NOTE

SECTION	PROJECT	SERIAL-CATEGORY	PAGE

SUBJECT: Figure 11 "Box" Geometry

NAME:

DATE:

REVISION DATE:

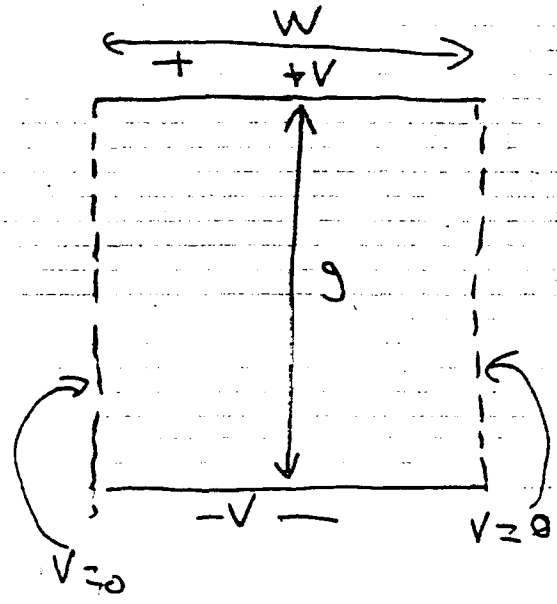

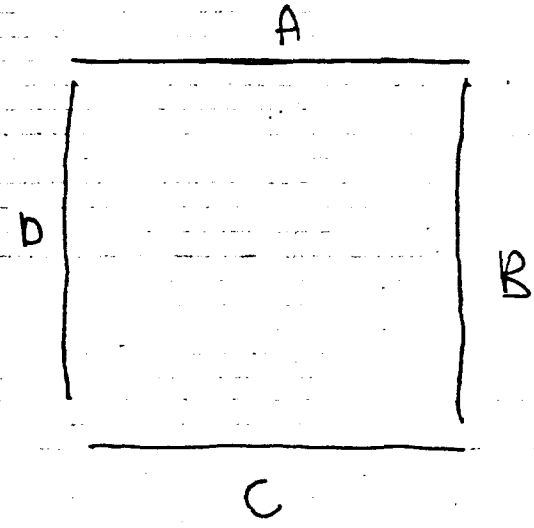

Box pickup

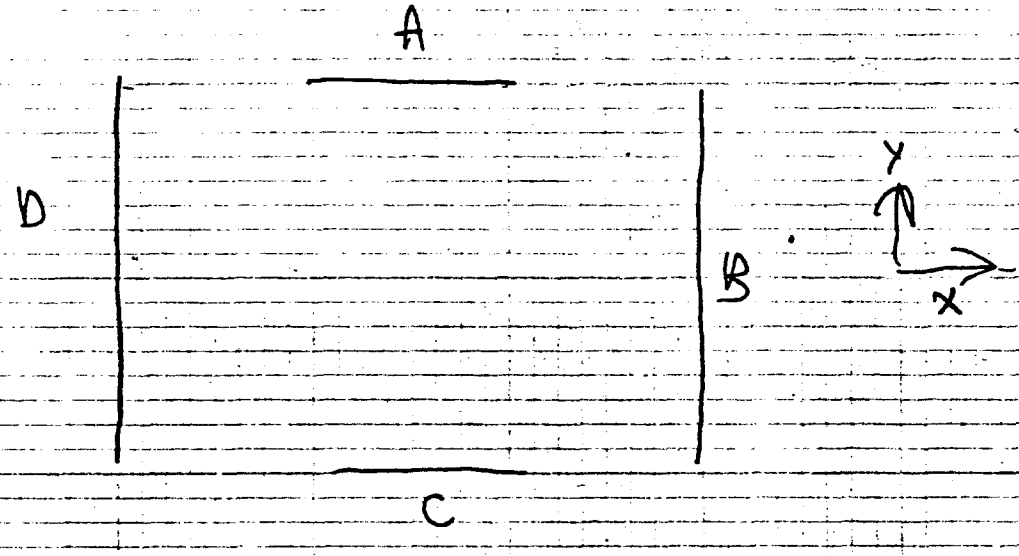

Possible ~~Pre Coo~~ Debuncher Coding Array

Fig 12 g = W Fields in "Box" geometry

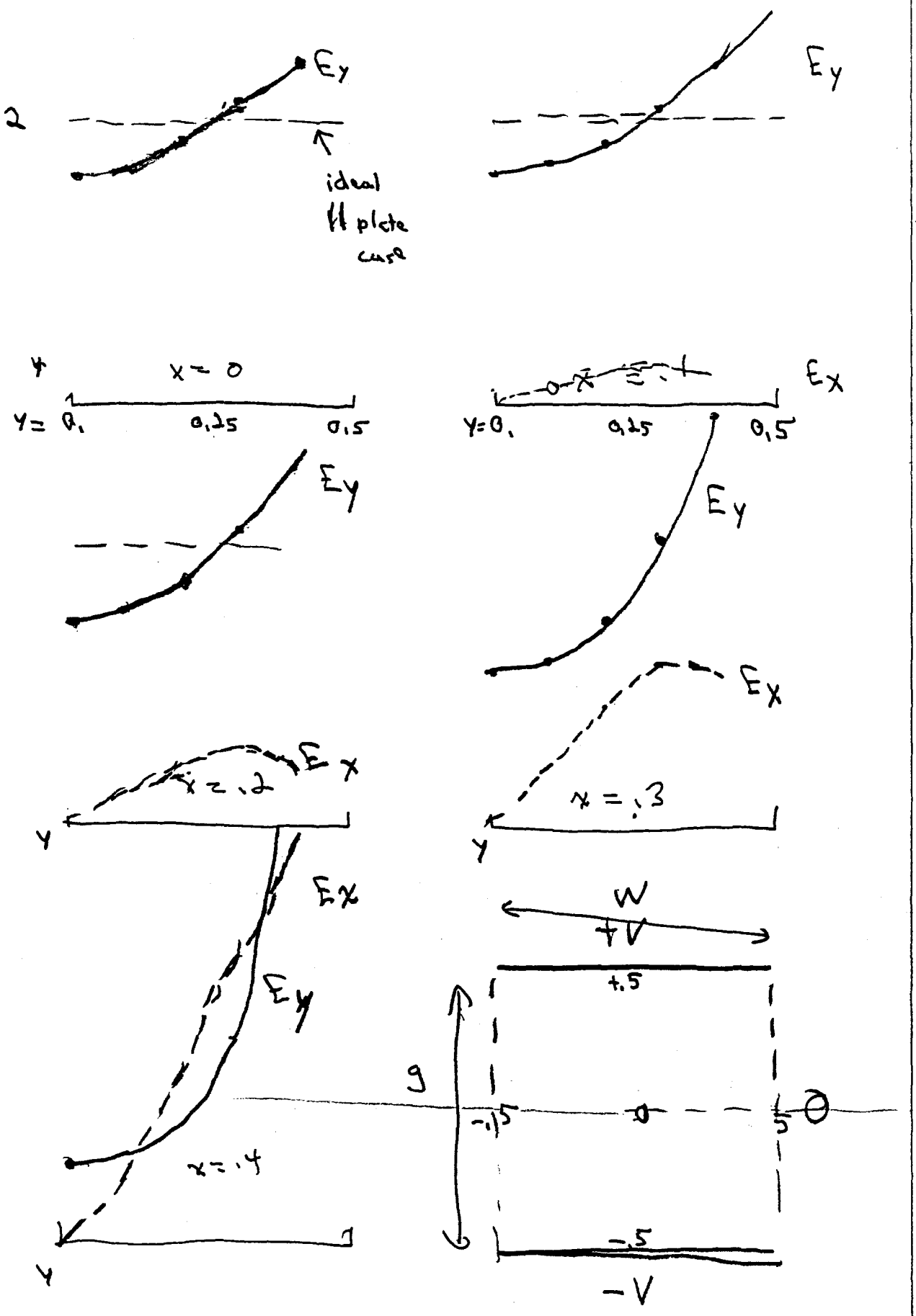
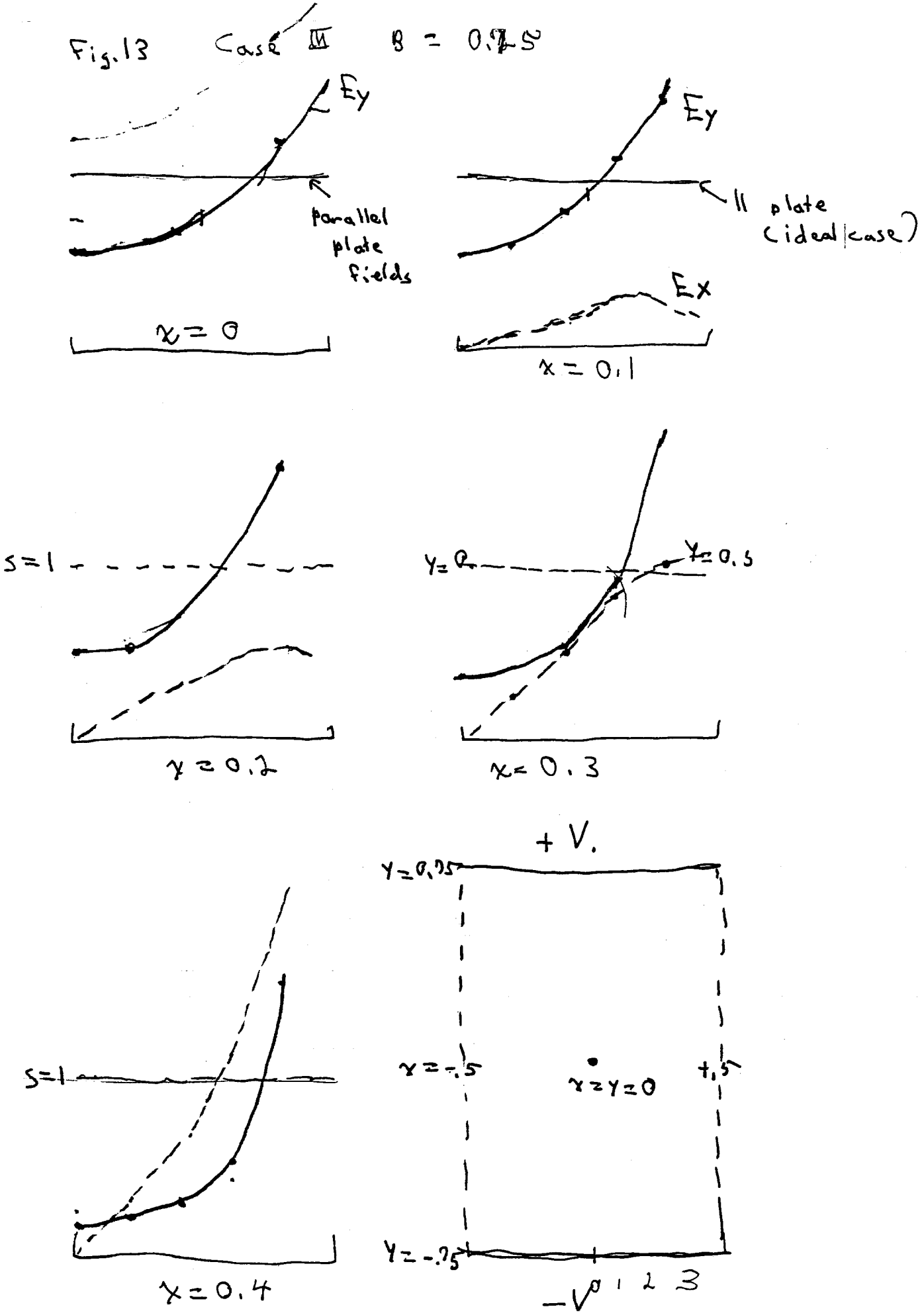
Fig. 13 Case III $\beta = 0.75$